*Journal of Molecular Recognition*

WILEY

Journal of Molecular Recognition

RESEARCH ARTICLE OPEN ACCESS

# Artificial Intelligence Clustering Approach for Force Mapping Analysis of Polyacrylic Acid (PAA)/Polyethylene Oxide (PEO) Polymer Brushes for Biosensor Applications

D. Saad[1,2] | F. Dubreuil[1] | A. Steinberger[3] | L. Calmettes[4] | E. Dellandrea[4] | M. Phaner-Goutorbe[2]

[1]Ecole Centrale de Lyon, LTDS, UMR5513, Ecully Cedex, France | [2]Ecole Centrale de Lyon, CNRS, INSA Lyon, Université Claude Bernard Lyon 1, CPE Lyon, INL, UMR5270, Ecully Cedex, France | [3]CNRS, ENS de Lyon, LPENSL, UMR5672, Lyon Cedex, France | [4]Ecole Centrale de Lyon, CNRS, Université Claude Bernard Lyon 1, INSA Lyon, Université Lumière Lyon 2, LIRIS, UMR5205, Ecully, France

**Correspondence:** M. Phaner-Goutorbe (magali.phaner@ec-lyon.fr)

**Received:** 8 December 2025 | **Revised:** 13 March 2026 | **Accepted:** 30 March 2026

**Keywords:** AFM | AI | clustering | force map | polymer brush

## ABSTRACT

Biocompatibility of a biosensor can be achieved by grafting polymer brushes onto a solid surface. These brushes must be able to attract specific analytes or repel unwanted entities. This is obtained with weak polyelectrolyte polymer brushes that shrink or swell depending on external stimuli. In this study, the conformation of polyacrylic acid (PAA) and polyethylene oxide (PEO) polymer brushes was characterized as a function of pH and ionic strength using Atomic Force Microscopy (AFM) in spectroscopic mode. Instead of colloidal tips classically used to measure the mechanical behavior of the brush, force curves were performed with conventional tips for better sensitivity to the interaction between ions and polymer, which is responsible for their conformation. Since force mapping experiments generate thousands of curves, a statistical representation was employed to define the general trend of the curves and facilitate their interpretation. As expected, the neutral PEO is not affected by changes in solution pH and salinity. In contrast, PAA exhibits behaviors depending on the ions present in the solution and increasing salinity; the brush shrinks at low pH with $H_3O^+$ ions and swells with the addition of $Na^+$ and $K^+$ ions. The originality of the study also lies in the implementation of an Artificial Intelligence (AI) clustering model applied to force curves to specifically study a 50% PAA/50% PEO mixed polymer brush. This AI model makes it possible to distinguish areas of the surface where only one type of polymer has been grafted and to identify its nature according to its force curve.

## 1 | Introduction

The surfaces of living cells, cartilage, and synovial joints are all composed of polyelectrolyte polymers. An artificial method for producing a biocompatible surface involves grafting a polymer brush onto a solid surface. This creates biologically active surfaces that play a crucial role in biosensors, tissue engineering, and other biomedical devices [1]. For biosensors, polymer films provide reproducible and stable platforms for the immobilization of various biomolecules to enable the recognition of target biomolecules in a given solution. However, to improve the sensitivity and selectivity of biosensors, it is important to prevent nonspecific binding of unwanted entities that would interfere with specific analyte binding [2]. Thus, a well-adapted biosensor should present controlled attractive and repelling polymer brushes on its bioactive surface.

A biosensor realized by a mixing of poly(ethylene oxide) (PEO) and poly(acrylic acid) (PAA) was considered a good candidate. The neutral PEO polymer is supposed to repel the entities when the negatively charged weak polyelectrolyte PAA is supposed to attract them under stimuli conditions. In fact, PAA is known to shrink or swell depending on the pH or the ionic strength of the solution [3, 4]. In the collapse conformation,

the entities are repelled. The conformation of both polymers deposited on different substrates such as gold and silicon was widely characterized by different techniques, such as Quartz Crystal Microbalance (QCM) [4], ellipsometry [5], total internal reflection fluorescence (TIRF) spectroscopy [6], and Atomic Force Microscopy (AFM) [7]. Dupont-Gillain et al. [4] have observed the adsorption of proteins in a mixed PEO/PAA brush system, governed by the swelling of PAA brushes, and their desorption, governed by their collapse, using QCM under selected pH and ionic strength. Ellipsometry was used by Currie et al. [5] to measure the thickness of PAA brushes, which increases with the swelling and decreases with the shrinking of the brushes, as a function of the pH, ionic strength and the grafting density. AFM force spectroscopy was also employed by Hoy et al. [7] to characterize the conformation of PAA brushes by analyzing hydrophobic interactions between the brushes and a silanized colloidal AFM probe using the obtained force-separation curves, where the separation is the tip-substrate distance.

This article proposes the study of the conformation of PEO and PAA polymers in six solutions of pH 5.5 and 7.4 with varying ionic strengths using AFM in force spectroscopy mode, by measuring force maps, that is to say sets of force-distance curves over a 2D grid on the polymer surface.

Conventional tips were used rather than colloidal probes to be more sensitive to the interaction of ions with the polymers than to the mechanical properties of the polymer brush and to achieve a better spatial resolution [8].

Since the process is stochastic, thousands of curves were generated during the experiments using a force map approach. A statistical representation was used to define the general trend of the curves and to facilitate their interpretation. In addition, an artificial intelligence learning model was developed to identify and localize on the force map the different behaviors among the curves. This model was applied to discriminate between the two polymers on a mixed PEO/PAA sample.

## 2 | Methods

### 2.1 | Polymer Brushes

Two polymers, the poly(acrylic acid) (PAA), a charged polyelectrolyte polymer, and the poly(ethylene oxide) (PEO), a neutral polymer, were studied after being grafted on an ultra-flat gold substrate using the "grafting onto" technique [9].

Poly(acrylic acid) (PAA) terminated with (α-thiol, ω-bromo) groups was purchased from Polymer Source, featuring an average molecular weight of Mn = 2000 g/mol (23 repeating units) and a polydispersity index of 1.3. Poly(ethylene oxide) (PEO) terminated with a methyl ether thiol group was purchased from Sigma-Aldrich. An average molecular weight of Mn = 2000 g/mol, was also chosen (43 repeating units) with a polydispersity index of 1.09.

Ultra-flat gold wafers Au(111) were purchased from Platypus Technologies [10]. These gold wafers, deposited on silicon substrates (gold thickness 100 nm), were used directly after being stripped from the template without further cleaning. These surfaces present an average RMS of 0.36 nm and large crystal grains of $3.64 \pm 0.2\,\mu m^2$.

The polymers were dissolved in Milli-Q water (resistivity of 18.2 MΩ cm) at a concentration of 1.5 g/L to yield pure solutions of PAA and PEO. These solutions were then deposited onto the ultra-flat gold surface and allowed to graft using "the grafting onto" method for a duration of 4 h to ensure optimal grafting density [11].

Additionally, a mixed 50% PAA/50% PEO sample was prepared by simultaneous grafting where a mixed polymer solution was prepared by mixing an equal amount of PAA and PEO solutions then deposited on a bare ultra-flat gold substrate following the aforementioned process.

To estimate this grafting density, a colorimetric method based on the selective binding of Toluidine Blue O (TBO) assay, a cationic dye, to the carboxyl groups of PAA is used [12]. An average grafting density of approximately $\sigma = 0.36 \pm 0.04$ chains $nm^{-2}$ is measured, which is considered "moderate" and optimal for our experimental conditions [13]. As this experiment was not possible on the neutral PEO brush, we have estimated in the rest of the article, a similar grafting density for PEO, or even slightly lower. Indeed, the greater length of the PEO chains (17.5 nm max) compared to the PAA chains (6.9 nm max) can lead to steric hindrance that can interfere with access to the surface.

### 2.2 | Solutions

For the experimental measurements, six solutions were prepared. Two solutions had varying pH levels: the first is 2 mL of Milli-Q water with 10 μL of 0.026 M HCl (at a pH of 5.5, ~$10^{-4}$ M HCl, for a Debye length of 26.6 nm) and the second 2 mL of diluted PBS (at a pH of 7.4, 0.01× PBS, ~$10^{-4}$ M $Na_2HPO_4$, for a Debye length of 7.4 nm). These solutions, named HCl and PBS solutions, were considered with very low salt concentration. Two high salt concentration solutions were prepared by adding 200 μL of 2 M NaCl to each of the aforementioned solutions thereby achieving a salt concentration of approximately 0.18 M and leading to Debye length of 0.7 nm each. Two moderate salt (0.02 M) solutions were also prepared by adding only 20 μL of 2 M NaCl to each of the aforementioned solutions. The six solutions are presented in Table 1.

Salt addition resulted in minimal pH variation in the solutions. After each measurement with salt, the samples were submerged in pure water for a couple hours before starting the next measurement to assure the total dissolution of any remaining salt

**TABLE 1** | The six solutions.

| | | | |
|---|---|---|---|
| pH = 5.5 | HCl | HCl + NaCl (0.02 M) | HCl + NaCl (0.18 M) |
| pH = 7.4 | PBS | PBS + NaCl (0.02 M) | PBS + NaCl (0.18 M) |

*Note:* Table representing the six solutions used in this study (pH and salt concentration).

particles on the surfaces. From one experiment to another, the pH value remained the same for buffered PBS solutions but it was able to vary for unbuffered HCl solutions, due to $CO_2$ absorption. Thus, fresh solutions were prepared before each experiment and regular pH measurements were taken yielding a value of $5.5 \pm 0.5$. Subsequently, we will consider a value of 5.5, while taking into account the uncertainty of the measurement and the possibility of a pH shift.

### 2.3 | AFM Force Spectroscopy

Experiments were performed using the AFM instruments NX10 from Park System using their open liquid cell chamber with a volume of liquid of about 2.3 mL, allowing to always maintain the sample and the tip in wet conditions during the experiments. Between two experiments, the fluid cell and the cantilever holder were rinsed with pure water to dissolve any remaining salt particles, and then with pure ethanol to remove any contamination.

A scan rate of 1 Hz per line and an approach and retract speed of 10 μm/s are chosen and the setpoint voltage was adjusted to 0.1 V corresponding to maximal forces between 10 and 20 nN. To facilitate comparison between curves, they were all cut at 10 nN.

FORTG (AppNano) cantilevers with a nominal stiffness between 1 and 2 $N\,m^{-1}$ were selected because their spring constant value, $k$, is high enough to limit the critical instability due to the attractive forces at small surface separations [14] but small enough to present a high sensitivity. Prior to each experiment, the cantilever was individually calibrated using the thermal noise method.

The cantilevers were made from silicon and back coated with gold. Colloidal tips are often used to measure the collective mechanical behavior of the brush layer caused by the tip. This parameter was voluntarily not considered and eliminated in our system. Thus, classical tips instead of colloidal large ones were used with a curvature radius below 14 nm (the value was overestimated as it was measured by imaging a tipcheck grid (Budget sensor) after force curves measurements). Their small radius makes it more efficient to detect hydration forces on the interface than electrostatic forces and achieve a better resolution [8, 15].

We have also decided to consider only the approach part of the force curves in this study since the way the tip pulls at the polymer brushes during retraction is off-topic. This article focuses primarily on the organization of these brushes on the studied surface. Although the retract curves were also recorded as Supporting Informations (Figure S1).

The measurement method exhibits a stochastic character due to various effects, the main ones being: thermal fluctuations of the tip and polymers, the spatial distribution of polymers under the tip for each measurement, and the variability of the position of ions and their charges along and between polymers. Therefore, it is necessary to generate a very large number of force curves to obtain reliable results.

Thus, the specific PinPoint mode, a force volume mapping mode available on the NX10, was used. A tip-surface interaction map is created by repeatedly acquiring the force-distance curve for each point on the surface. Then, each measurement corresponds to a $32 \times 32$ pixels square force map, covering a $25 \times 25$ nm area and containing 1024 force curves. To ensure the consistency and reliability of our data and curves, between 5 and 10 force maps were acquired for each sample at different locations. Numerous samples of pure PAA, pure PEO, and 50%/50% PAA/PEO mixtures were studied in six different solutions. Of these, 10 were selected for analysis due to their reproducibility. This represents a global dataset of approximately 300,000 curves (10 significant samples × 5 force maps (min) × 6 solutions × 1024 curves/map). All these curves were compared, and an average curve was calculated for each sample-solution system. In order to simplify our presentation, we have chosen in this article the most representative force curve for each sample-solution system, that is, the one whose set of 1024 curves most closely approximated the corresponding average curve, in order to illustrate each of the three samples and six solutions.

The variability and homogeneity of the 1024 curves was evaluated in a specific force map, using a statistical representation. The 1024 force versus separation curves were superimposed and presented as 2D force-separation histograms [16, 17], where the yellow color indicates a high density of similar data points, and dark blue indicates a low density (Figure 1a). A low variability of the curves was observed, demonstrating the high repeatability of the measurements, with great homogeneity. Thus, a median force-separation curve was extracted for each measurement, which will be used further to discuss the different interaction processes (Figure 1b).

Finally, neither the average nor the median is suitable for characterizing the differences between the two polymers in the mixed sample. To address this limitation, we developed a machine learning model to process the set of curves from each measurement and automatically classify them into groups based on their similarities. In this study, an unsupervised learning approach—specifically clustering—was adopted to automatically organize the data so that the elements within each group (or cluster) are more similar to each other than to those in other groups. A cluster can therefore be viewed as a homogeneous and compact collection of objects that share common characteristics while differing from objects in other clusters.

The agglomerative hierarchical clustering (AHC) algorithm [18] was chosen because it is deterministic and does not require specifying the number of clusters in advance. The algorithm works by successively grouping curves according to increasing proximity. It begins by assuming that each curve is an individual class and then iteratively merges the two closest groups according to the chosen distance function (Euclidean distance in this study). This process continues until all curves are merged into a single group. The result is a hierarchy of partitions—nonoverlapping subsets of the original dataset that together include all data points—which can be visualized using a dendrogram as Supporting Informations (Figure S2). In this dendrogram, each of the 1024 curves in the dataset is represented along the $x$-axis, while the $y$-axis indicates the distance at which two instances or clusters are joined. The height of the connecting link corresponds to this distance: a large jump denotes a significant dissimilarity between groups.

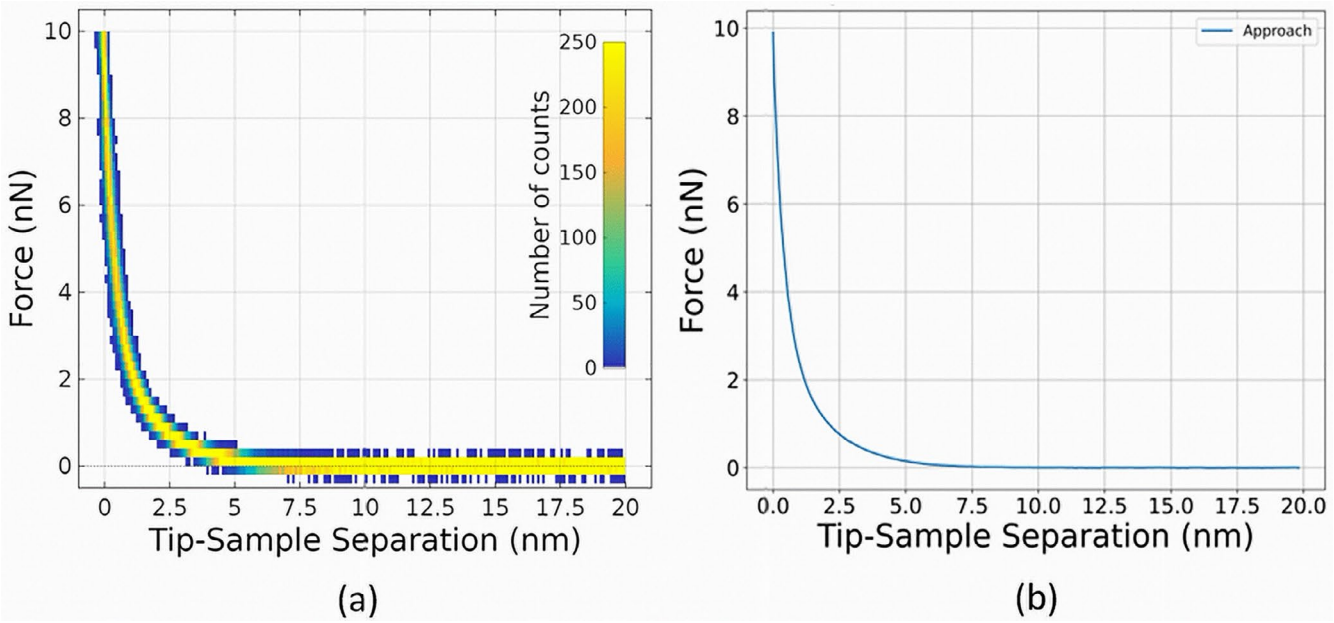


**FIGURE 1** | Approach part of the AFM force-separation curve for PAA in PBS + NaCl (0.18 M), shown as (a) a 2D histogram and (b) the corresponding median force curve extracted from it.

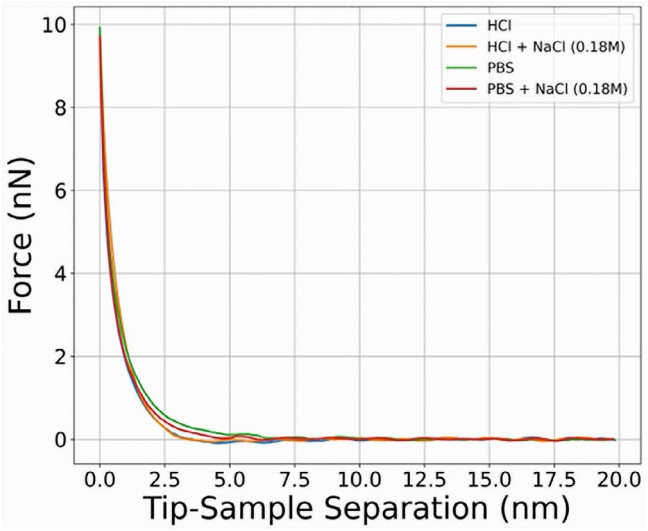


**FIGURE 2** | Influence of pH and salt concentration in PEO. Median AFM force-separation curves of PEO in the four solutions: HCl, HCl + NaCl (0.18 M), PBS, and PBS + NaCl (0.18 M).

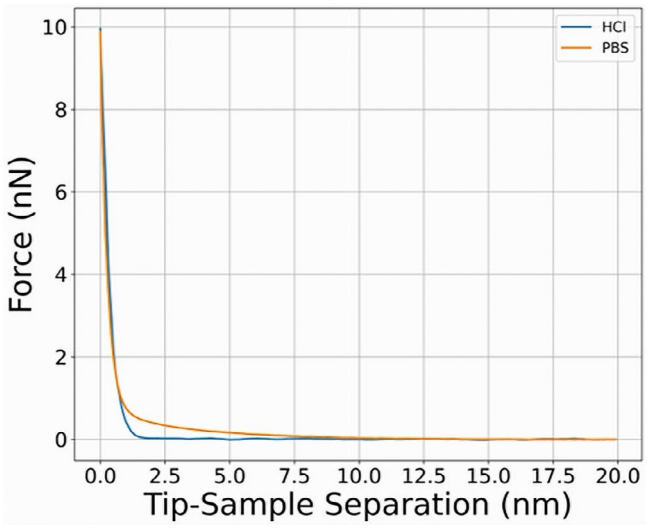


**FIGURE 3** | Influence of the pH on PAA. Median AFM force-separation curves of PAA in the two low concentrated solutions: HCl and PBS.

The optimal cut of the dendrogram can thus be determined by identifying such discontinuities, ensuring that data within clusters remain similar while clusters themselves are clearly distinct.

## 3 | Results and Discussion

### 3.1 | PEO Brush

PEO is a neutral polymer with uncharged chains [19]. Thus, variations in pH or ionic strength are not expected to modify the brush conformation. This is exactly what is observed on Figure 2. The force-distance curves obtained in the four solutions, HCl, PBS, HCL + NaCl (0.18 M), and PBS + NaCl (0.18 M) are globally very close to each other.

They all present a repulsive behavior that extends from 5 to 7 nm, smaller than the maximal length of our PEO molecule (~17.5 nm) but different to the one obtained on the PAA brush surface (Figure 3).

As the PEO is neutral, its elongation is dependent on the van-der-Waals interaction between chains and then on the proximity between them. For a grafting density lower than 0.36 molecules $nm^{-2}$, as expected, the van-der-Waals interaction is weak and the chains adopt a random conformation between collapsing and stretching: a *ruffled* brush that does not extend longer than 7 nm.

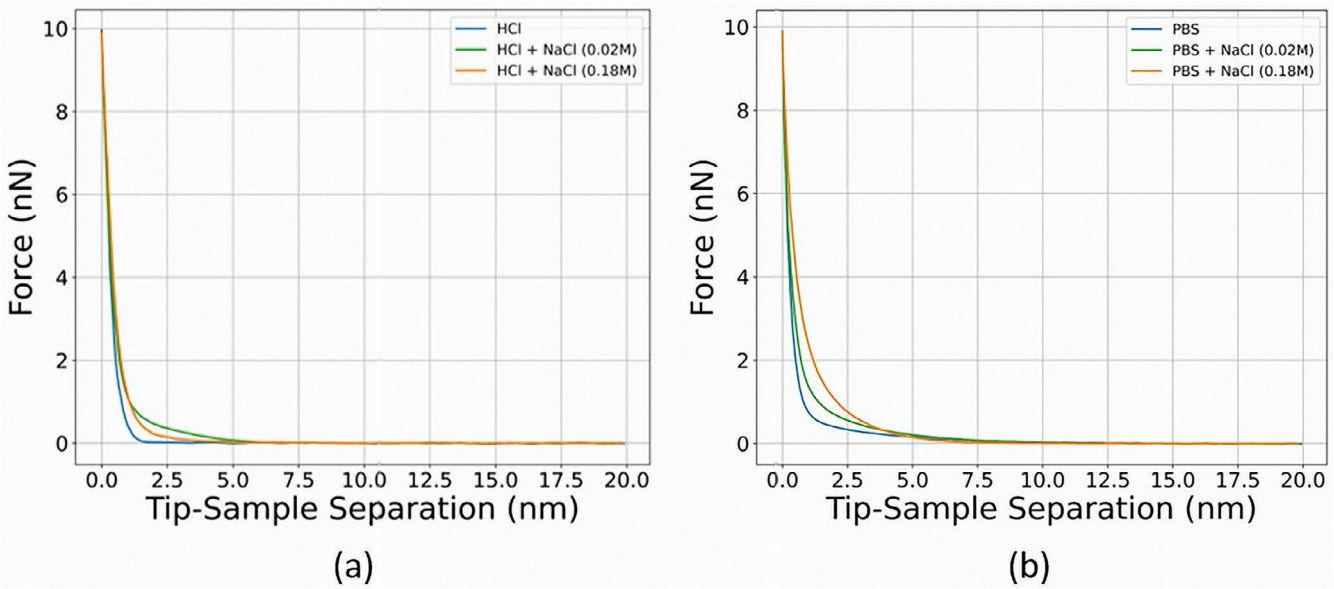


**FIGURE 4** | Influence of the salt concentration in PAA. Median AFM force-separation curves of PAA (a) in the 3 HCl solutions: HCl, HCl + NaCl (0.02 M), HCl + NaCl (0.18 M) and (b) in the 3 PBS solutions: PBS, PBS + NaCl (0.02 M), and PBS + NaCl (0.18 M).

The average force-separation curves on PEO display a slight ondulation for separations above 7 nm that is below the noise level on individual curves (see Supporting Informations (Figure S3)). This modulation, accentuated by the superposition of the different curves, seems to be specific to the PEO systems, as it is not visible in the average curves on the PAA brushes. Since it occurs in the region between 7 nm and the maximal extension of the PEO molecules, it might be due to some very weak interaction between the AFM tip and the PEO molecules in this region, but this very subtle feature is beyond the scope of this paper.

**TABLE 2** | ($\Delta z$) detected interaction distance.

| Solution | HCl | HCl + NaCl (0.02 M) | HCl + NaCl (0.18 M) |
|---|---|---|---|
| $\Delta z$ (nm) | 1.78 ± 0.05 | 6.31 ± 0.05 | 4.10 ± 0.05 |
| **Solution** | **PBS** | **PBS + NaCl (0.02 M)** | **PBS + NaCl (0.18 M)** |
| $\Delta z$ (nm) | 7.03 ± 0.05 | 7.35 ± 0.05 | 6.66 ± 0.05 |

*Note:* Table summarizing the separation distance at which interaction is first detected ($\Delta z$) in the six solutions for the PAA sample.

## 3.2 | PAA Brush

### 3.2.1 | Impact of the pH

Figure 3 presents the median approach force-distance curves obtained in the two low salt solutions: HCl and PBS. Both curves are different and demonstrate the influence of the pH solution on the polymer conformation.

PAA is classified as a weak polyelectrolyte, because its carboxylic acid groups can ionize in aqueous solutions. The percentage of ionized carboxylic acid groups is defined by the degree of dissociation ($\alpha$) [20]. It was shown that this ($\alpha$) value is very difficult to evaluate properly in the brush layer structure as it depends on the "apparent $pK_a$ value" [20], the local pH in the brush [21–23], the concentration of added salt and the local polymer concentration [24].

From titration curves measurements [25], we can establish that for a pH at 5.5, the PAA brushes have a degree of ionization $\alpha$ of around 0.5, that is, 50% of their carboxylic groups are ionized or protonated, whereas at a pH of 7.4, $\alpha$ is around 0.9 meaning that the majority of the polymer brushes are ionized. When the polymer molecules are ionized they can repel each other, leading to an extended configuration of the polymer. This can explain the difference between the repulsive force at a pH of 5.5 and 7.4.

In our curves, we can determine two parameters (Figures 3 and 4). First, we can examine the shape of the curve which should provide information about the strength of the interaction (not studied in this paper). Second, we can extract the distance at which the force becomes superior to the fluctuation at large distances, $\Delta z$. This $\Delta z$ value corresponds to the distance at which the tip begins to feel the interaction with the polymer and all the ionic environment, so it is related to the extension of the polymer and its surrounding ions in the solution (Table 2). It should be noted that the measured $\Delta z$ distance is close to the Debye Length value for the PBS solution (7.4 nm), but very far from it for the other solutions (26.6 nm in HCl and 0.7 nm in HCl + NaCl (0.18 M) and PBS + NaCl (0.18 M)). This confirms the idea that the electrostatic force due to organization of ions in solution is not accessible in our study due to the fineness of our tips. On the other hand, our force curves reflect the impact of ions on the organization of polymer chain [8, 15].

At a pH of 5.5, the repulsive force on PAA starts at 2 nm (blue curve on Figure 3) and is sharper than on PEO (Figure 2). As

the PAA molecule is smaller than the PEO one and as only 50% of the carboxylic groups are ionized, the protonation of the other groups reduces the interaction between the polymer chain. Therefore, the chains adopt more of a collapsed shape than an extended shape on the gold surface. At a pH of 7.4, the curve increases slightly from 8 to 0.5 nm and then more abruptly until contact (orange curve on Figure 3), following the curve at a pH of 5.5 for very low separations. The shape of the curve at a pH of 7.4 is very different from the one at a pH of 5.5 in the region between 1 and 8 nm, with another slope and a higher repulsive (positive) force. The carboxylic groups are mostly negatively charged (90%), meaning that electrostatic repulsions between the chains are high and lead to the elongation of the brush. However, the repulsive force extends to 8 nm, which is slightly above the maximum possible length of the PAA molecule. Therefore, it seems that our sharp tip is sensitive not only to the polymer brush structure but also to the organization of the ions from the PBS surrounding the polymer [8].

#### 3.2.2 | Impact of the Ionic Strength

In the literature, two different regimes are described the impact of salt on the behavior of polyelectrolyte brushes [3, 5, 23]. First, the osmotic regime, typically observed at low salt concentrations (below 0.1 M), the concentration of the negatively charged PAA chains (due to deprotonation) keeps positive counterions $H_3O^+$ confined within the brush layer. The resulting electrostatic interaction between $COO^-$ charged groups inside the brush increases leading to the stretching and swelling of the polymer chains.

The second regime is the salted brush regime where the high amount of added salt ions, specifically the positive cations, screen the electrostatic interactions between the polymer $COO^-$ groups. More ions are condensed inside the polymer brush, reaching a concentration similar to the one in the bulk solution [21]. Electrostatic repulsions between charged groups are reduced and cause the collapse of the chain with the increase of the salt concentration [5].

In our study, we do not really observe the collapse of the chain at high salinity; therefore, an intermediate concentration was investigated. Figure 4a,b illustrates the impact of the ionic strength with force-distance curves obtained with different concentrations of NaCl salt: 0 M, 0.02 M, and 0.18 M at the two pH. The distance at which the force becomes nonzero, $\Delta z$, is reported on Table 2. We noticed that this distance is greatest at intermediate concentration. This nonmonotonic behavior of polyelectrolyte brushes at low or moderate ionic strength has already been reported in the literature [5, 21, 22] for longer PAA chains. Prior to significant collapse, polymer brushes can exhibit an initial swelling under moderate salt concentration. This occurs when external $Na^+$ ions enter the brush layer, replacing $H_3O^+$ ions, leading to an increase of the local pH. This process induces a higher dissociation of the COOH groups in the chains, allowing the polymer chains to extend and causing the brush to expand before it eventually collapses at much higher salt concentrations [5, 26, 27].

However, it was reported that for short polymer chains (as in our case), the brush conformation becomes less sensitive to pH change, and no pH-induced swelling is typically observed [28]. Moreover, shorter PAA chains are known to be locally stiffer than longer ones [29], which limits their ability to undergo conformational changes such as pH-induced swelling or salt-induced collapse. The fact that such changes are still detectable in our measurements, even if only slightly, highlights the high sensitivity of our characterization technique.

#### 3.2.3 | 50% PAA/50% PEO Mixed Polymer

Clear differences between PAA and PEO were observed in the median force curves measured in our study. This suggests that our measurements are well adapted to discriminate polymer type, PAA or PEO, in a system with unknown proportion of grafted polymers. To further explore this idea, we prepared an additional sample consisting of a 50% PAA/50% PEO mixed polymer and measured it by AFM spectroscopy. We expected to detect the characteristic force signatures of both polymers in the sample system.

The mixed sample was measured in the six different solutions with varying pH (pH at 5.5 and 7.4) and ionic strength (0 M, 0.02 M, and 0.18 M), but only the result concerning the HCl + 0.02 M NaCl solution is illustrated in Figure 5.

The 2D histogram of Figure 5a presents a higher dispersity and lower homogeneity compared to the pure individual PAA and PEO sample, as expected for a mixed 50% PAA/50% PEO brush sample. Two distinct turquoise curves corresponding to two sets of concentrated data points can be observed. These two types of curves can be clearly identified: one resembling those obtained for pure PAA and the other similar to those of pure PEO in the same solution (Figure 5b).

In addition, the coexistence of PAA-like and PEO-like behaviors in the mixed sample was further evidenced through the clustering method (Figure 5b,c). The dendrogram (Figure S2) suggests a partition of the curves into three clusters represented in green, red, and orange. The identification of the polymer type was performed by comparing the median force curves of the pure polymer samples (PAA and PEO) (Figure 5b) with the $32 \times 32$ clustered curves of the mixed sample (Figure 5c). One curve corresponds to one pixel of the color map that covers a $25 \times 25\,nm^2$ area (Figure 5d). Thus, for this small area, the map clearly reveals a heterogeneity of the polymers' spatial distribution. We can see orange and green zones that refer to PAA and PEO regions, respectively. The red intermediate curves are mostly measured at the limit between the two green and orange zones or sometimes dispersed. The red cluster can describe either interactions with both polymers at the limit of the zone or some isolated different type of polymers inside the zone (some PAA polymers in a PEO zone for example or the opposite).

The AI clustering approach appears to be an efficient tool to help us identify, thanks to the curves' shape, the nature of the polymers in the different zones.

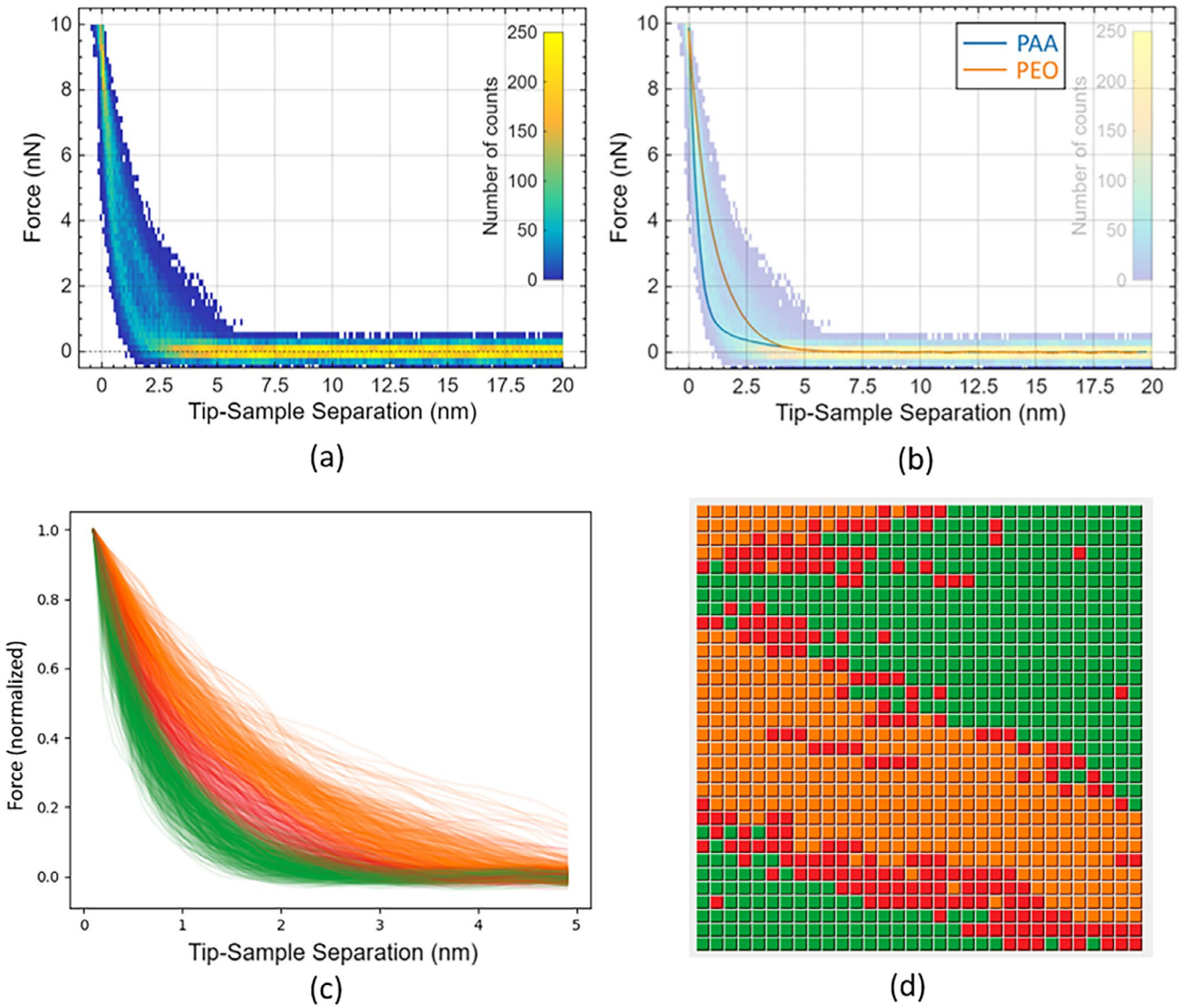


**FIGURE 5** | Mixed 50/50 PEO/PAA Polymers in the HCl + NaCl (0.02 M) solution: (a) 2D histogram of the AFM force-separation curve, (b) corresponding median force curve in pure PAA and pure PEO superposed on the 2D histogram, (c) representation of the 1024 curves categorized by the AI clustering program, with the following color-code: Cluster 1 in orange, cluster 2 in green, cluster 3 in red, (d) corresponding color map of 32 × 32 points on 25 × 25 nm with the same color code.

### 3.3 | Limitations of the Study

In order to improve the accuracy of our results, we plan to optimize the stability of the medium by using buffered solutions in acidic conditions. This approach will eliminate any pH drift and strengthen the robustness of our experimental data.

To enrich this study, our field of investigation will be extended to a wider range of pH and ionic strengths by exploring various salts.

Furthermore, to enhance analytical depth, we are transitioning from Agglomerative Hierarchical Clustering (AHC) toward the implementation of high-performance neural network architectures.

## 4 | Conclusion

Overall, these results demonstrate that AFM force spectroscopy with a sharp tip instead of a colloidal tip, combined with statistical analysis using 2D histograms, is a powerful approach for analyzing and understanding the behavior of polymer brushes in solution, particularly with respect to changes in pH and salt concentration, as it is very sensitive to minute changes in the brush configuration. As expected, the neutral PEO polymer was not perturbed by changes in the pH and in the salinity of the solution and adopted a ruffled conformation according to our moderate grafting density.

In contrast, the weak polyelectrolyte PAA has shown different behaviors depending on the pH of the solution and the salinity despite its short size. It appears that the PAA brush collapses at a

pH of 5.5 when surrounded by $H_3O^+$ ions and swells with adding other ions in the salted solutions. In PBS, the PAA brush is in a swollen configuration due to a higher dissociation of the polymer at a pH of 7.4. We also observed, as previously mentioned by Currie et al. [5] and Chu et al. [27] that the polymer brush extension is more important in intermediate salt solution than in higher salted concentration. In PBS, our results showed that the added salt modifies not only the chain extension but also the repulsive force within the brush in a way that remains to be understood by further studies.

Finally, our AI clustering analysis of the mixed PAA/PEO sample has proved to be adapted to discriminate areas on the surfaces where only one type of polymer has been grafted.

These results are very encouraging as they demonstrate that it is possible to create and to identify areas with different polymers at the scale of individual polymers. This is really promising for the development of biosensors with polymer brushes with different affinities toward proteins or bacteria.

### Author Contributions

All authors have read and approved the final manuscript. D.S., F.D, A.S, L.C., E.D., and M. Phaner-Goutorbe performed the research. F.D. and M. Phaner-Goutorbe designed the research study. D.S. contributed to acquisition of force curves. L.C. contributed to implementation of IA Clustering model. D.S., F.D., A.S., L.C., E.D., and M. Phaner-Goutorbe contributed to analysis the data and writing and review the paper. M. Phaner-Goutorbe editing.


### Acknowledgments

We greatly acknowledge Rémi de Maistre and Aicha Outlit who have participated to the implementation of the IA clustering model in collaboration with Léo Calmettes. Open access publication funding provided by COUPERIN CY26.

### Funding

The authors thank Ecole centrale de Lyon for financial support for D.S. PhD grants.


### Ethics Statement

The authors have nothing to report.

### Consent

The authors have nothing to report.

### Conflicts of Interest

The authors declare no conflicts of interest.

### Data Availability Statement

The data that support the findings of this study are openly available in Recherche Data Gov repository at https://doi.org/10.57745/12KVNP.

### References


1. J. M. Goddard and J. H. Hotchkiss, "Polymer Surface Modification for the Attachment of Bioactive Compounds," *Progress in Polymer Science* 32, no. 7 (2007): 698–725, https://doi.org/10.1016/J.PROGPOLYMSCI.2007.04.002.

2. C. Zhao, L. Y. Li, M. M. Guo, and J. Zheng, "Functional Polymer Thin Films Designed for Antifouling Materials and Biosensors," *Chemical Papers* 66, no. 5 (2012): 323–339, https://doi.org/10.2478/S11696-012-0147-1/METRICS.

3. X. Guo and M. Ballauff, "Spherical Polyelectrolyte Brushes: Comparison Between Annealed and Quenched Brushes," *Physical Review E* 64, no. 5 (2001): 051406, https://doi.org/10.1103/PhysRevE.64.051406.

4. M. F. Delcroix, S. Demoustier-Champagne, and C. C. Dupont-Gillain, "Quartz Crystal Microbalance Study of Ionic Strength and pH-Dependent Polymer Conformation and Protein Adsorption/Desorption on PAA, PEO, and Mixed PEO/PAA Brushes," *Langmuir* 30, no. 1 (2014): 268–277, https://doi.org/10.1021/la403891k.

5. E. P. K. Currie, A. B. Sieval, G. J. Fleer, and M. A. C. Stuart, "Polyacrylic Acid Brushes: Surface Pressure and Salt-Induced Swelling," *Langmuir* 16, no. 22 (2000): 8324–8333, https://doi.org/10.1021/la991528o.

6. O. Hollmann and C. Czeslik, "Characterization of a Planar Poly(Acrylic Acid) Brush as a Materials Coating for Controlled Protein Immobilization," *Langmuir* 22, no. 7 (2006): 3300–3305, https://doi.org/10.1021/LA053110Y.

7. O. Hoy, B. Zdyrko, R. Lupitskyy, et al., "Synthetic Hydrophilic Materials With Tunable Strength and a Range of Hydrophobic Interactions," *Advanced Functional Materials* 20, no. 14 (2010): 2240–2247, https://doi.org/10.1002/ADFM.201000170.

8. A. Halperin and E. B. Zhulina, "Atomic Force Microscopy of Polymer Brushes: Colloidal Versus Sharp Tips," *Langmuir* 26, no. 11 (2010): 8933–8940, https://doi.org/10.1021/la9047374.

9. N. Akkilic and W. M. de Vos, "Responsive Polymer Brushes for Biomedical Applications," in *Switchable and Responsive Surfaces and Materials for Biomedical Applications* (Wood Head Publishing, 2015), 119–146, https://doi.org/10.1016/B978-0-85709-713-2.00005-5.

10. "Platypus Technologies Ultra-Flat Gold Film," accessed August 30, 2024, https://www.platypustech.com/gold-thin-films/ultra-flat-gold-films.

11. M. F. Delcroix, G. L. Huet, T. Conard, et al., "Design of Mixed PEO/PAA Brushes With Switchable Properties Toward Protein Adsorption," *Biomacromolecules* 14, no. 1 (2013): 215–225, https://doi.org/10.1021/bm301637h.

12. A. Rangel, T. N. Nguyen, and V. Migonney, "Choice of Parameters for Toluidine Blue O Colorimetric Assay: Influence on the Determination of Grafting Density of Anionic Groups," *Journal of Applied Spectroscopy* 89, no. 3 (2022): 552–558, https://doi.org/10.1007/S10812-022-01394-6/METRICS.

13. N. R. Hollingsworth, S. I. Wilkanowicz, and R. G. Larson, "Salt- and pH-Induced Swelling of a Poly(Acrylic Acid) Brush via Quartz Crystal Microbalance w/Dissipation (QCM-D)," *Soft Matter* 15, no. 39 (2019): 7838–7851, https://doi.org/10.1039/C9SM01289C.

14. A. C. Hillier, S. Kim, and A. J. Bard, "Measurement of Double-Layer Forces at the Electrode/Electrolyte Interface Using the Atomic Force Microscope: Potential and Anion Dependent Interactions," *Journal of Physical Chemistry* 100, no. 48 (1996): 18808–18817, https://doi.org/10.1021/jp961629k.

15. S. R. Van Lin, K. K. Grotz, I. Siretanu, N. Schwierz, and F. Mugele, "Ion-Specific and pH-Dependent Hydration of Mica-Electrolyte Interfaces," *Langmuir* 35, no. 17 (2019): 5737–5745, https://doi.org/10.1021/ACS.LANGMUIR.9B00520/ASSET/IMAGES/LARGE/LA-2019-00520F_0005.JPEG.

16. J. M. Black, D. Walters, A. Labuda, et al., "Bias-Dependent Molecular-Level Structure of Electrical Double Layer in Ionic Liquid on Graphite," *Nano Letters* 13, no. 12 (2013): 5954–5960, https://doi.org/10.1021/NL4031083.

17. L. Bou Tannous, M. Simoes Santos, Z. Gong, et al., "Effect of Surface Chemistry on the Electrical Double Layer in a Long-Chain Ionic

Liquid," *Langmuir* 39, no. 47 (2023): 16785–16796, https://doi.org/10.1021/acs.langmuir.3c02123.

18. D. Müllner, "Modern Hierarchical, Agglomerative Clustering Algorithms," September 2011, accessed November 21, 2025, https://arxiv.org/pdf/1109.2378.

19. W. Liu and E. M. Nestorovich, "Probing Protein Nanopores With Poly(Ethylene Glycol)s," *Proteomics* 22, no. 5–6 (2022): e2100055, https://doi.org/10.1002/PMIC.202100055.

20. K. Ehtiati, S. Z. Moghaddam, A. E. Daugaard, and E. Thormann, "How Dissociation of Carboxylic Acid Groups in a Weak Polyelectrolyte Brush Depend on Their Distance From the Substrate," *Langmuir* 36, no. 9 (2020): 2339–2348, https://doi.org/10.1021/acs.langmuir.9b03537.

21. V. Senechal, H. Saadaoui, N. Vargas-Alfredo, J. Rodriguez-Hernandez, and C. Drummond, "Weak Polyelectrolyte Brushes: Re-Entrant Swelling and Self-Organization," *Soft Matter* 16, no. 33 (2020): 7727–7738, https://doi.org/10.1039/D0SM00810A.

22. J. Hur, K. N. Witte, W. Sun, and Y.-Y. Won, "On the Origins of the Salt-Concentration-Dependent Instability and Lateral Nanoscale Heterogeneities of Weak Polyelectrolyte Brushes: Gradient Brush Experiment and Flory-Type Theoretical Analysis," *Langmuir* 26, no. 3 (2010): 2021–2034, https://doi.org/10.1021/la902549b.

23. T. Wu, P. Gong, I. Szleifer, P. Vlček, V. Šubr, and J. Genzer, "Behavior of Surface-Anchored Poly(Acrylic Acid) Brushes With Grafting Density Gradients on Solid Substrates: 1. Experiment," *Macromolecules* 40, no. 24 (2007): 8756–8764, https://doi.org/10.1021/MA0710176/SUPPL_FILE/MA0710176SI20070701_083727.PDF.

24. H. Zhang and J. Rühe, "Swelling of Poly(Methacrylic Acid) Brushes: Influence of Monovalent Salts in the Environment," *Macromolecules* 38, no. 11 (2005): 4855–4860, https://doi.org/10.1021/ma047501f.

25. U. Kim and W. M. Carty, "Effect of Polymer Molecular Weight on Adsorption and Suspension Rheology," *Journal of the Ceramic Society of Japan* 124, no. 4 (2016): 484–488, https://doi.org/10.2109/jcersj2.15219.

26. J. D. Willott, T. J. Murdoch, F. A. M. Leermakers, and W. M. De Vos, "Behavior of Weak Polyelectrolyte Brushes in Mixed Salt Solutions," *Macromolecules* 51, no. 3 (2018): 1198–1206, https://doi.org/10.1021/ACS.MACROMOL.7B02244/ASSET/IMAGES/LARGE/MA-2017-022449_0008.JPEG.

27. X. Chu, J. Yang, G. Liu, and J. Zhao, "Swelling Enhancement of Polyelectrolyte Brushes Induced by External Ions," *Soft Matter* 10, no. 30 (2014): 5568–5578, https://doi.org/10.1039/C4SM00860J.

28. T. Swift, L. Swanson, M. Geoghegan, and S. Rimmer, "The pH-Responsive Behaviour of Poly(Acrylic Acid) in Aqueous Solution Is Dependent on Molar Mass," *Soft Matter* 12, no. 9 (2016): 2542–2549, https://doi.org/10.1039/C5SM02693H.

29. D. G. Mintis and V. G. Mavrantzas, "Effect of pH and Molecular Length on the Structure and Dynamics of Short Poly(Acrylic Acid) in Dilute Solution: Detailed Molecular Dynamics Study," *Journal of Physical Chemistry B* 123, no. 19 (2019): 4204–4219, https://doi.org/10.1021/ACS.JPCB.9B01696.

## Supporting Information

Additional supporting information can be found online in the Supporting Information section. **Figure S1:** Ten superimposed forces-distance curves: approach (blue) and retract (orange) parts of (a) PAA and (b) PEO in HCl $10^{-4}$ M solution. **Figure S2:** Dendrogram of clustering results for the mixed sample in HCl + NaCl (0.02 M). **Figure S3:** Extraction of 1 force curve among a set of 1024 curves for PEO (a) in HCl $10^{-4}$ M solution and (b) in HCl + NaCl (0.18 M), (c) in PBS, (d) in PBS + NaCl (0.18 M).